

in the δ 1.0–1.5 range for *n*-pentyl. The integration of the singlet to multiplet is the expected 5:11. The UV–visible absorption exhibits a shoulder at 250, a maximum at 310 (ϵ 2700 M⁻¹ cm⁻¹ in isoctane), and a shoulder at 350 nm.

- (3) (a) Hoffman, N. W.; Brown, T. L. *Inorg. Chem.* **1978**, *17*, 613. These authors suggest W–H cleavage by light, initiating radical substitution processes. Preliminary results in our laboratory show evidence that dissociative loss of CO is a significant result of optical excitation of $(\eta^5\text{-C}_5\text{H}_5)\text{W}(\text{CO})_3\text{H}$. (b) Bainbridge, A.; Craig, P. J.; Green, M. *J. Chem. Soc. A* **1968**, 2715.
- (4) Severson, R. G.; Wojcicki, A. *J. Organomet. Chem.* **1978**, *157*, 173.
- (5) We find that PPh₃ reacts with $(\eta^5\text{-C}_5\text{H}_5)\text{W}(\text{CO})_2(1\text{-pentene})\text{H}$ to yield $(\eta^5\text{-C}_5\text{H}_5)\text{W}(\text{CO})_2(\text{PPh}_3)(n\text{-pentyl})$. Presumably, the reaction occurs as a result of the reversion of the alkene–hydride to the alkyl followed by scavenging by PPh₃. Rate of reaction as a function of PPh₃ concentration supports this mechanism. The approximate rate of conversion of $(\eta^5\text{-C}_5\text{H}_5)\text{W}(\text{CO})_2(1\text{-pentene})\text{H}$ into $(\eta^5\text{-C}_5\text{H}_5)\text{W}(\text{CO})_2(n\text{-pentyl})$ is $\sim 2 \times 10^{-3} \text{ s}^{-1}$ at 25 °C. The slow rate may be due to the fact that the alkene–hydride is the trans isomer.
- (6) (a) Alway, D. G.; Barnett, K. W. *Adv. Chem. Ser.* **1978**, No. 168, 115. (b) Mills, W. C., III; Wrighton, M. S. *J. Am. Chem. Soc.* **1979**, *101*, 5830. (c) Geoffroy, G. L.; Wrighton, M. S. "Organometallic Photochemistry"; Academic Press: New York, 1979.
- (7) Low-temperature infrared data were obtained using a Cryogenics Technology Incorporated Spectrum II cryocooler using a sample compartment equipped with NaCl windows. Paraffin solutions of $(\eta^5\text{-C}_5\text{H}_5)\text{W}(\text{CO})_3\text{R}$ were prepared by heating the paraffin to the melting point (~ 70 °C) and dissolving the complex. The solution was then coated onto sapphire flats and mounted in the cryocooler for irradiation and spectroscopic measurements.

Romas J. Kazlauskas, Mark S. Wrighton*

Department of Chemistry
Massachusetts Institute of Technology
Cambridge, Massachusetts 02139

Received October 22, 1979

Heterodinuclear Di- μ -sulfido Bridged Dimers Containing Iron and Molybdenum or Tungsten. Structures of $(\text{Ph}_4\text{P})_2(\text{FeMS}_2)$ Complexes (M = Mo, W)

Sir:

Molybdenum K-edge X-ray absorption fine structure (EXAFS) analyses have been reported for the MoFe protein components of the *Clostridium pasteurianum*¹ and *Azotobacter vinelandii*² (*Az. v.*) nitrogenases, and for the FeMo cofactor² (FeMo-co) from *Az. v.*³ These studies have led to the conclusion that the Mo coordination environments are very similar, and in all cases the Mo is coordinated by three or four S atoms at 2.3 Å and is at close proximity (<3 Å) to two or three Fe atoms.

A partial adherence to the above coordination requirements for the Mo atom is found in the structures of the "double cubane" cluster complexes $[\text{Mo}_2\text{Fe}_6\text{S}_9(\text{SEt})_8]^{3-4}$ and $[\text{Mo}_2\text{Fe}_6\text{S}_8(\text{SR})_9]^{3-}$ (R = Et;⁴ R = Ph;⁵ R = SCH₂CH₂OH⁶). The EXAFS spectra of the Mo centers in the ethyl derivatives of these clusters are very similar to those obtained for the nitrogenase systems.⁴ Because of basic differences in the Mo:Fe:S atom ratios between the FeMo proteins, the FeMo-co, and the "double cubanes", the latter cannot be considered complete analogues. However, it seems likely that Mo-containing fragments in the "double cubanes" may be identical with fragments in FeMo-co and the nitrogenases.⁴

In our approach to the construction of Mo–Fe–S clusters in appropriate Mo:Fe ratios we have initiated synthetic efforts toward the isolation of molecular "building blocks" that contain Fe, S, and Mo, which eventually may be used in the synthesis of clusters of higher complexity. In a recent publication we reported⁷ on the synthesis and structural characterization of one such molecule, $(\text{Et}_4\text{N})_2[(\text{PhS})_2\text{FeS}_2\text{MoS}_2]^{2-}$ (I) (Figure 1). In this communication we report on the tungsten analogue of this complex, $[(\text{PhS})_2\text{FeS}_2\text{WS}_2]^{2-}$ (II), and the reactions of I and II with trisulfides. The complex II was obtained by the reaction of $[\text{WS}_4]^{2-}$ with an equimolar amount of $[\text{Fe}(\text{SPh})_4]^{2-}$ ⁸ in dimethylformamide (DMF) and isolated, in near-quantitative yields, as red crystals of the Ph_4P^+ or

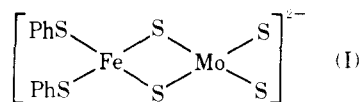


Figure 1.

Et_4N^+ salts, upon addition of diethyl ether to the DMF solutions. Anal. Calcd for $\text{WFeS}_6\text{C}_{60}\text{H}_{50}\text{P}_2$: C, 56.96; H, 3.98; S, 15.2; Fe, 4.41. Found: C, 56.92; H, 4.01; S, 15.09; Fe, 4.40. The visible spectrum (DMF) of this paramagnetic compound ($\mu_{\text{eff}}^{\text{corr}} = 4.73 \mu_{\text{B}}$ at 298 K) is characterized by absorptions at 540 nm (sh), 466 (sh), 432 (ϵ 6890), 409 (11 300), and 375 (8310). Single-crystal diffraction patterns of the Et_4N^+ salt of II are very similar to those of I and show that the two complexes are isomorphous and very likely isostructural. An $S = 2$ ground state is suggested by the magnetic moment of II, and the simple Curie–Weiss magnetic behavior, evident in the temperature dependence of the isotropically shifted proton resonances,⁹ rules out the population of higher spin states at a temperature as high as 352 K. The ⁵⁷Fe Mössbauer spectrum of II at 4.2 K shows a single doublet with a quadrupole splitting (QS) of 2.24 (1) mm/s and an isomer shift (IS) of 0.48 (1) mm/s (relative to Fe metal at 298 K). These values are similar to those obtained for I at 4.2 K (QS, 1.96 (1); IS, 0.45 mm/s) and suggest that the electronic environment of the Fe atom is rather insensitive to a change from Mo to W in the heterodinuclear dimers. By Mössbauer, isomer shift criteria established for the iron–sulfur proteins and their synthetic analogues, a value of +0.45 mm/s is intermediate between those observed for high-spin Fe(II) and Fe(III) in tetrahedral sulfur environments.¹⁰

The reactions of the Ph_4P^+ salts of either I or II with 10 equiv of R₃SSR (R = C₇H₇) in warm DMF proceed readily. Upon cooling and dilution with absolute ether, these DMF solutions deposit X-ray isomorphous crystals of the $(\text{Ph}_4\text{P})_2[(\text{S}_5)\text{FeS}_2\text{MS}_2]$ salts as the hemi-DMF solvates (M = Mo, dark brown crystals, 86% yield; M = W, dark red crystals, 79% yield). Anal. Calcd for $\text{FeMoS}_9\text{C}_{48}\text{H}_{40}\text{P}_2 \cdot \frac{1}{2}(\text{C}_7\text{H}_7\text{ON})$ (III): C, 51.44; H, 3.80; N, 0.61; P, 5.36; S, 24.97; Mo, 8.30. Found: C, 50.62; H, 3.84; N, 0.64; P, 5.22; S, 24.23; Mo, 8.43. Anal. Calcd for $\text{FeWS}_9\text{C}_{48}\text{H}_{40}\text{P}_2 \cdot \frac{1}{2}(\text{C}_7\text{H}_7\text{ON})$ (IV): C, 47.56; H, 3.54; N, 0.56; S, 23.32; Fe, 4.51. Found: C, 46.75; H, 3.25; N, 0.41; S, 21.9. Electronic spectra for IV: 550 nm (ϵ 1250), 464 (sh), 425 (7480), 398 (7830), 366 (9390). The magnetic moments ($\mu_{\text{eff}}^{\text{corr}}$) of III and IV, 4.90 and 4.90 μ_{B} at 298 K, respectively, again indicate $S = 2$ ground states for these complexes. The Mössbauer spectrum of IV (in liquid N₂) consists of a single doublet and shows a quadrupole splitting of 1.66 (1) mm/s and an isomer shift of 0.51 (1) mm/s.

Single crystal, X-ray diffraction, intensity data on III and IV were collected on a Picker-Nuclear FACS-I automatic diffractometer using a θ – 2θ scan technique.¹¹ The data corrected for Lorentz, polarization, and absorption effects were used for the solution of the structures by conventional Patterson and Fourier techniques. Refinement by full-matrix least-squares methods has progressed to conventional $R = 9.5\%$ for III and 8.5% for IV using isotropic thermal parameters for the carbon atoms and the DMF-solvate molecule and anisotropic thermal parameters for all other atoms. The hydrogen atoms have not been included in the refinement process as yet. The structures of the anions (Figure 2) show the tetrahedrally coordinated Fe atoms bound by S_5^{2-} bidentate chelates and by the MS_4^{2-} (M = Mo, W) units which also serve as bidentate chelates. The S_5^{2-} anion, although not a common ligand, occurs as a bidentate chelate in $[\text{Fe}_2\text{S}_{12}]^{2-}$,¹² $(\text{PtS}_{15})^{2-}$,¹³ and $\text{Ti}(\text{Cp})_2\text{S}_5$.¹⁴ In the structures of $[\text{Fe}_2\text{S}_{12}]^{2-}$ and $(\text{PtS}_{15})^{2-}$, the MS_5 "ring" units are found in the chair conformation

Table I. Selected Structural Parameters in the $[(S_5)FeS_2MS_2]^{2-}$ Complexes ($M = Mo, W$) and $[(PhS)_2FeS_2MoS_2]^{2-}$ *a, b*

	$M = Mo$	$M = W$	$[(PhS)_2FeS_2MoS_2]^{2-}$
Bond Lengths, Ångstroms			
Fe-M	2.731 (3)	2.753 (3)	2.750 (4)
M-S _{T1}	2.139 (6)	2.142 (6)	2.148 (6)
M-S _{T2}	2.151 (7)	2.172 (8)	2.159 (6)
M-S _{B1}	2.261 (7)	2.240 (6)	2.247 (6)
M-S _{B2}	2.244 (5)	2.269 (7)	2.245 (6)
Fe-S _{B1}	2.253 (7)	2.260 (7)	2.242 (7)
Fe-S _{B2}	2.236 (6)	2.280 (7)	2.258 (7)
Fe-S ₁	2.347 (8)	2.329 (9)	2.303 (7)
Fe-S ₅	2.296 (6)	2.309 (7)	2.320 (7)
S _{1B} -S _{2B}	3.568 (8)	3.588 (6)	3.571 (8)
S ₁ -S ₅	3.822 (9)	3.865 (6)	
Bond Angles, Degrees			
S ₁ -M-S ₅ ^c	109.4 (2.7) ^d	109.4 (2.2) ^f	109.2 (2.4) ^h
S ₁ -Fe-S ₅ ^c	109.3 (6.3) ^e	109.2 (6.6) ^g	109.4 (6.2) ⁱ
Fe-S _B -M ^c	74.3 (3)	74.9 (6)	75.5 (2)

^a From ref 7. ^b For all structures the reported structural parameters are in analogous reference to the labeling shown in Figure 2. ^c Mean values; the standard deviation from the mean are in parenthesis. ^d Range, 104.8 (3) to 111.8 (3)°. ^e Range 99.3 (3) to 117.2 (3)°. ^f Range 105.4 (2) to 110.9 (3)°. ^g Range 99.2 (3) to 117.6 (3)°. ^h Range 104.5 (3) to 116.6 (3)°. ⁱ Range 102.9 (3) to 116.9 (3)°.

similar to the conformation found for the FeS₅ "ring" in the present structures. Selected structural parameters in the $[FeMS_5]^{2-}$ anions are shown¹⁵ in Table I and are compared with corresponding values in the structure of the $[(PhS)_2FeS_2MoS_2]^{2-}$ anion. The FeS₂M units are essentially planar and very similar to the one found in the structure of I. The terminal M-S₁ bond lengths are significantly shorter than the M-S₅ lengths; however, they still are longer than "typical" M=S bonds. Terminal Mo-S bonds are found in the range 2.085–2.129 Å.¹⁶

The mean Fe-S₁ bond lengths in III and IV, 2.321 and 2.319 Å, respectively, are appreciably shorter than the mean Fe-S bond length in $[Fe(SPh)_4]^{2-}$, 2.355 (14) Å,¹⁷ and quite similar to the mean Fe-S₁ bond lengths in $[Fe_2S_2(S_2-p\text{-tolyl})_4]^{2-}$, 2.312 (1) Å,¹⁸ which formally contains Fe(III).

A choice between two of the reasonable descriptions for the formal oxidation states of the two metal ions in the heterodinuclear dimers [Fe(II)-M(VI) vs. Fe(III)-M(V)] cannot be made on the basis of the available spectroscopic and magnetic data. A $S = 2$ ground state for these molecules can arise from either (a) a high-spin Fe(II) ($S = 2$) mixed ligand complex, SFeL, [$S = 2PhS^-$ or S_2^{2-} ; $L = MS_4^{2-}$, $M = Mo(VI)$ or $W(VI)$] or (b) a high-spin Fe(III) ion ($S = 5/2$) in the dimer strongly coupled to a Mo(V) or W(V) ($S = 1/2$) ion in a reduced MS₄ unit. The rather short Mo-Fe distances [2.750 (4) and 2.731 (3) Å] found in the structures of I and III, respectively, and a W-Fe distance of 2.753 Å in IV cannot be considered as concrete evidence for Fe-Mo or Fe-W bonding [and a Fe(III)-M(V) description]. In the linear trimeric molecule, $[Cl_2FeS_2MoS_2FeCl_2]^{2-}$, where Mössbauer and magnetic data show¹⁹ the presence of Fe(II), the Mo-Fe distances are equally short. A structure invariant in these μ -sulfido bridged molecules seems to be the acute M-S-Fe bridge angle of ~ 74 – 76° which controls the distance of the M-Fe separation.²⁰

The electronic spectrum of III (Figure 3) [605 nm (ϵ 1864), 545 (sh), 480 (7242), 410 (9924), 305 (14,894)] is dominated by absorptions that originate from the MoS₄ chromophore and is similar, but hypsochromically shifted, relative to the spectrum of I [620 nm (sh), 550 (sh), 487 (ϵ 8645), 425 (7773), 330 (14 705)].

A similar electronic absorption spectral pattern is observed in the spectra of acid-treated, reneutralized solutions of the Fe-Mo protein from *Clostridium pasteurianum* (Figure 2

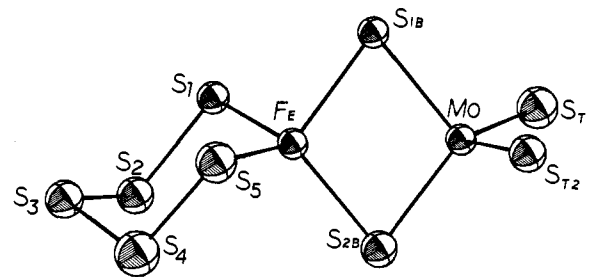


Figure 2. Structure and labeling of the $[(S_5)FeS_2MS_2]^{2-}$ anions ($M = Mo, W$). Thermal ellipsoids as drawn by ORTEP (C. K. Johnson, ORNL-3794, Oak Ridge National Laboratory, Oak Ridge, Tenn., 1965) represent the 50% probability surfaces.

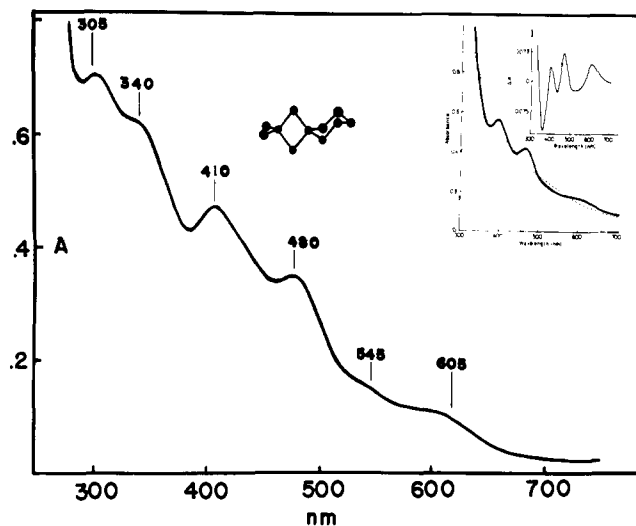


Figure 3. The visible spectrum of $(Ph_4P)_2[(S_5)FeS_2MoS_2]$ in DMF. Inset: the visible spectrum, in water, of acid-treated reneutralized Fe-Mo protein from *Clostridium pasteurianum* from ref 21.

inset). Chromatography on these solutions allows for the isolation of a fraction with a visible spectrum identical with that of aqueous MoS_4^{2-} .²¹ The formation of MoS_4^{2-} from components released under the reported experimental conditions does not seem likely. Instead it appears that MoS_4^{2-} is a component of the nitrogenase Fe-Mo-S site and is released following acid hydrolysis.

The electronic perturbations of the MoS_4^{2-} chromophore apparent in the spectra of I and (III) between 500 and 300 nm must arise from the MoS_4^{2-} -Fe coordination. Similar perturbations are observed in the spectra of the acid-base-treated Fe-Mo protein solutions and could be attributed to MoS_4^{2-} -Fe interactions.²² These interactions also could account for the low energy bands at ~ 620 and ~ 540 nm. Such low energy absorptions are observed in the spectra of I (620, 550 nm) and III (605, 545 nm) and very likely arise from Fe-S charge transfer processes.

Acknowledgments. This work has been generously supported by grants from the National Science Foundation (CHE-79-0389), the National Institutes of Health (GM 26671-01) and a NATO Research Grant (No. 1321). The computing expenses have been covered by grants from the University of Iowa, Graduate College.

Supplementary Material Available: Structure factors for the $(Ph_4P)_2[(S_5)FeS_2MS_2]$ complexes ($M = Mo, W$) and positional coordinates for $(Ph_4P)_2[(S_5)FeS_2WS_2]$ (38 pages). Ordering information is given on any current masthead page.

References and Notes

- S. P. Cramer, K. O. Hodgson, W. O. Gillum, and L. E. Mortenson, *J. Am. Chem. Soc.*, **100**, 3398 (1978).

- (2) S. P. Cramer, W. O. Gillum, K. O. Hodgson, L. E. Mortenson, E. I. Stiefel, J. R. Chisnell, W. J. Brill, and V. K. Shah, *J. Am. Chem. Soc.*, **100**, 3814 (1978).
- (3) V. K. Shah and W. J. Brill, *Proc. Natl. Acad. Sci. U.S.A.*, **74**, 3249 (1977).
- (4) (a) T. E. Wolff, J. M. Berg, C. Warrick, K. O. Hodgson, R. H. Holm, and R. B. Frankel, *J. Am. Chem. Soc.*, **100**, 4630 (1978); (b) T. E. Wolff, J. M. Berg, K. O. Hodgson, R. B. Frankel, and R. H. Holm, *ibid.*, **101**, 4140 (1979).
- (5) (a) G. Christou, C. D. Garner, F. E. Mabbs, and T. J. King, *J. Chem. Soc., Chem. Commun.*, 740 (1978); (b) G. Christou, C. D. Garner, and F. E. Mabbs, *Inorg. Chim. Acta*, **28**, L189 (1978).
- (6) G. Christou, G. D. Garner, F. E. Mabbs, and M. G. B. Drew, *J. Chem. Soc., Chem. Commun.*, 91 (1979).
- (7) D. Coucouvanis, E. D. Simhon, D. Swenson, and N. C. Baenziger, *J. Chem. Soc., Chem. Commun.*, 361 (1979).
- (8) D. G. Holah and D. Coucouvanis, *J. Am. Chem. Soc.*, **97**, 6917 (1975).
- (9) NMR spectra ($\text{Me}_2\text{SO}-d_6$, 298 K) show the *m*-H resonance at 36.64 downfield and the *p*-H resonance 35.94 ppm upfield from Me_4Si in a 2:1 intensity ratio. The assignments were made on the basis of the *p*- CH_3 substituted phenyl ring derivative. The *o*-H resonance could not be detected, very likely because of extensive broadening. The magnitude of the shifts decreases as temperature is increased over the range 294–352 K.
- (10) See for example ref 4b (Figure 7).
- (11) Crystal and refinement data for $(\text{Ph}_4\text{P})_2\text{FeMoS}_9 \cdot \frac{1}{2}\text{DMF}$: cell dimensions, $a = 11.874$ (3), $b = 22.486$ (5), $c = 10.698$ (3) Å; $\alpha = 107.3$ (1), $\beta = 79.27$ (3), $\gamma = 106.86$ (4)°; space group, $P1$; $Z = 2$; $d_{\text{calcd}} = 1.43$ g cm^{-3} , $d_{\text{obsd}} = 1.44$ g cm^{-3} ; crystal dimensions, $0.2 \times 0.04 \times 0.3$ mm; $2\theta_{\text{max}}$, 40° (Mo radiation); reflections used, $F^2 > 3\sigma(F^2)$, 3110; unique reflections, 4902; parameters, 330. Crystal and refinement data for $(\text{Ph}_4\text{P})_2\text{FeWS}_9 \cdot \frac{1}{2}\text{DMF}$: cell dimensions $a = 11.882$ (7), $b = 22.487$ (20), $c = 10.707$ (7) Å; $\alpha = 107.0$ (1), $\beta = 78.93$ (5), $\gamma = 107.16$ (7)°; space group, $P1$, $Z = 2$; $d_{\text{calcd}} = 1.54$ g cm^{-3} , $d_{\text{obsd}} = 1.55$ g cm^{-3} ; crystal dimensions, $0.1 \times 0.2 \times 0.04$ mm; $2\theta_{\text{max}}$, 40° (Mo radiation); reflections used, $F^2 > 3\sigma(F^2)$, 3236; unique reflections, 4505; parameters, 330.
- (12) D. Coucouvanis, D. Swenson, P. Stremple, and N. C. Baenziger, *J. Am. Chem. Soc.*, **101**, 3392 (1979).
- (13) P. E. Jones and L. Katz, *Acta Crystallogr., Sect. B*, **25**, 745 (1969).
- (14) H. Köpf, B. Block, and M. Schmidt, *Chem. Ber.*, **101**, 272 (1968).
- (15) The DMF molecules of solvation are found with half occupancy at the center of symmetry, $\frac{1}{2}, \frac{1}{2}, 0$.
- (16) J. T. Huneke and J. H. Enemark, *Inorg. Chem.*, **17**, 3698 (1978).
- (17) D. Coucouvanis, D. Swenson, N. C. Baenziger, D. G. Holah, A. Kostikas, A. Simopoulos, and V. Petrouleas, *J. Am. Chem. Soc.*, **98**, 5721 (1976).
- (18) J. J. Mayerle, S. E. Denmark, B. V. De Pamphilis, J. A. Ibers, and R. H. Holm, *J. Am. Chem. Soc.*, **97**, 1032 (1975).
- (19) D. Coucouvanis, N. C. Baenziger, E. D. Simhon, P. Stremple, D. Swenson, A. Simopoulos, A. Kostikas, V. Petrouleas, and V. Papaefthymiou, *J. Am. Chem. Soc.*, following paper in this issue.
- (20) Very recently we have obtained the crystalline $(\text{Ph}_4\text{P})_2[(\text{PhS})_2\text{CoS}_2\text{MS}_2]$ complexes ($M = \text{Mo}, \text{W}$). These complexes are X-ray isomorphous to the analogous iron complexes and show electronic spectra typical of tetrahedrally coordinated cobalt(II).
- (21) W. G. Zumft, *Eur. J. Biochem.*, **91**, 354 (1978).
- (22) These interactions do not survive the chromatographic procedure which results in the isolation of MoS_4^{2-} .

D. Coucouvanis,* N. C. Baenziger
E. D. Simhon, P. Stremple, D. Swenson
Department of Chemistry, University of Iowa
Iowa City, Iowa 52242

A. Kostikas, A. Simopoulos
V. Petrouleas, V. Papaefthymiou
Nuclear Research Center "Demokritos"
Aghia Paraskevi, Attiki, Greece
Received October 29, 1979

Synthesis and Structural Characterization of the $(\text{Ph}_4\text{P})_2[\text{Cl}_2\text{FeS}_2\text{MS}_2\text{FeCl}_2]$ Complexes ($M = \text{Mo}, \text{W}$). First Example of a Doubly Bridging MoS_4 Unit and Its Possible Relevance as a Structural Feature in the Nitrogenase Active Site

Sir:

In a preceding communication¹ we reviewed the structural information available for the Mo site in nitrogenases. This information, obtained on the basis of Mo X-ray absorption fine structure (EXAFS) analyses, has led to the suggestion that a valid structural model for the Mo site of nitrogenase must involve two major features: a set of three or four Mo bound sulfur atoms at $\sim 2.36 \pm 0.02$ Å and a set of two (or three?) iron

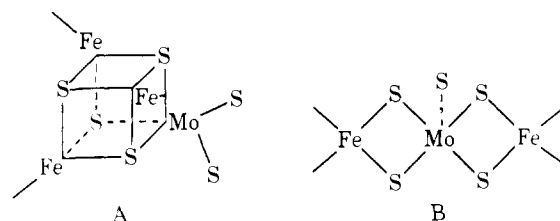


Figure 1.

atoms at a distance of 2.72 ± 0.03 Å from the Mo. Of the two distinct models, proposed for the nitrogenase Mo site² (Figure 1), A exists as a fragment in the recently synthesized and structurally characterized "double cubanes".³ In this communication we report on the synthesis and structural characterization of a heteronuclear Fe–Mo–Fe linear trimer and the tungsten analogue. The former, at least partly, resembles B' (Figure 1).

The reaction of the $(\text{Ph}_4\text{P})_2[(\text{SPh})_2\text{FeS}_2\text{MS}_2]$ complexes⁴ ($M = \text{Mo}, \text{W}$) with $\text{FeCl}_3 \cdot 6\text{H}_2\text{O}$ in 1:2 molar ratio in dimethylformamide (DMF) results in the oxidation of the ^-SPh ligands to PhSSPh with the concomitant generation of Fe(II) ions. From the DMF solutions, upon the addition of ether, crystalline, X-ray isomorphous $(\text{Ph}_4\text{P})_2[\text{Cl}_2\text{FeS}_2\text{MS}_2\text{FeCl}_2]$ complexes can be isolated [$M = \text{Mo}$, brown crystals 67% yield (I); $M = \text{W}$, orange-red crystals, 60% yield (II)]. Anal. Calcd for $\text{Fe}_2\text{MoCl}_4\text{S}_4\text{P}_2\text{C}_{48}\text{H}_{40}$: C, 49.85; H, 3.49; P, 5.36; S, 11.09; Cl, 12.26; Fe, 9.66. Found: C, 49.69; H, 3.42; P, 5.36; S, 10.94; Cl, 11.60; Fe, 9.30. Anal. Calcd for $\text{Fe}_2\text{WCl}_4\text{S}_4\text{P}_2\text{C}_{48}\text{H}_{40}$: C, 46.34; H, 3.24; S, 10.30; W, 14.77; Cl, 11.39. Found: C, 46.23; H, 3.32; S, 10.35; W, 14.45; Cl, 11.57.

The ⁵⁷F Mössbauer spectrum of I at 4.2 K shows a single doublet with a quadrupole splitting (QS) of 1.99 (1) mm/s and an isomer shift (IS) of 0.58 (1) mm/s (relative to Fe metal at 298 K). These values, and particularly the isomer shift, are not very similar to those obtained¹ for the $[(\text{SPh})_2\text{FeS}_2\text{MS}_2]^{2-}$ complexes ($M = \text{Mo}, \text{W}$). The IS in I, however, has a value close to that reported for the $\text{Fe}(\text{SC}_6\text{H}_5)_4^{2-}$ complex⁵ (0.66 mm/s) and for the FeS_4 sites in reduced rubredoxins⁶ (0.65 mm/s). These observations suggest that the two iron atoms in I are in the +2 formal oxidation state. The magnetic moment for I ($\mu_{\text{eff}}^{\text{corr}} = 6.635$ (2) μ_B at 300 K) is lower than that expected for two, noninteracting, high-spin ($S = 2$) Fe(II) ions in I. A temperature-dependence study of the magnetic susceptibility, however, shows typical antiferromagnetic behavior. Similar magnetic properties are observed with II ($\mu_{\text{eff}}^{\text{corr}} = 6.03$ (2) μ_B).

Crystal and refinement data for the structure of I are shown in Table I. Intensity data were obtained on a Picker FACS I automatic diffractometer using a step-scan technique, employing graphite monochromatized Mo $K\alpha$ radiation ($\lambda = 0.7107$ Å, $2\theta_m = 12.2^\circ$). The data were corrected for Lorentz and polarization effects and for absorption. The structure was solved by conventional Patterson and Fourier techniques and refined by full-matrix least-squares calculations. All atoms in the anion and the two phosphorus atoms were refined with anisotropic temperature factors. The carbon atoms in the cations were refined with isotropic temperature factors. The hydrogen atoms were included in the structure factor calculation at their calculated positions ($\text{C-H} = 0.95$ Å) but were not refined. Structural details for the complex anion are shown in Table II.

A nearly linear, Fe–Mo–Fe, array is found in the structure of the anion (Figure 2) in which the MoS_4^{2-} unit bridges two terminal FeCl_2 moieties. The MoS_4 and FeCl_2S_2 fragments show distorted tetrahedral geometry around the metal atoms. The mean value⁷ for the two independent Fe–Mo distances [2.775 (6) Å] is slightly greater than the Fe–Mo distances in $[\text{FeMoS}_9]^{2-}$ (III) and $[(\text{SC}_6\text{H}_5)_2\text{FeS}_2\text{MoS}_2]^{2-}$ (IV), 2.731